Monatsh Chem (2010) 141:1273–1278
DOI 10.1007/s00706-010-0403-4

ORIGINAL PAPER

On the chemical synthesis of titanium nanoparticles from ionic liquids

Ayi A. Ayi · Varsha Khare · Peter Strauch · Jérôme Girard · Katharina M. Fromm · Andreas Taubert

Received: 17 March 2010 / Accepted: 12 September 2010 / Published online: 7 October 2010

Abstract We report on attempts towards the synthesis of titanium nanoparticles using a wet chemical approach in imidazolium-based ionic liquids (ILs) under reducing conditions. Transmission electron microscopy finds nanoparticles in all cases. UV/Vis spectroscopy confirms the nanoparticulate nature of the precipitate, as in all cases an absorption band between ca. 280 and 300 nm is visible. IR spectroscopy shows that even after extensive washing and drying, some IL remains adsorbed on the nanoparticles. Raman spectroscopy suggests the formation of anatase nanoparticles, but X-ray diffraction reveals that, possibly, amorphous titania forms or that the nanoparticles are so small that a clear structure assignment is not possible. The report thus shows that (possibly amorphous) titanium oxides even form under reducing conditions and that the chemical synthesis of titanium nanoparticles in ILs remains elusive.

A. A. Ayi · V. Khare · P. Strauch · A. Taubert (✉)
Institute of Chemistry, University of Potsdam,
Karl-Liebknecht-Str. 24–25, Building 26,
144766 Golm, Germany
e-mail: ataubert@uni-potsdam.de

V. Khare · A. Taubert
Max Planck Institute of Colloids and Interfaces,
14476 Golm, Germany

J. Girard · K. M. Fromm
Department of Chemistry, University of Fribourg,
1700 Fribourg, Switzerland

Present Address:
A. A. Ayi
Materials Chemistry Unit, Department of Pure and Applied Chemistry, University of Calabar, P.M.B. 1115 Calabar, Nigeria

Keywords Ionic liquids · Nanoparticles · Titanium · Titanium oxide · Chemical reduction

Introduction

Nanoparticles are interesting owing to their optical, magnetic, and catalytic properties and thus their resulting applications in chemical technology, magnetic data storage, and sensing, to name a few examples [1]. As a result, an enormous number of studies have been devoted to the development of suitable protocols for the targeted and rational synthesis of inorganic nanoparticles, their stabilization, properties, processing, and application [2–8]. The main issue very often is the synthesis and stabilization of one specific particle size, particle morphology, or crystal phase. Besides aqueous and organic solvents [7–14], ionic liquids (ILs) have also recently been explored as reaction media and stabilizers for inorganic nanoparticle synthesis [15–26]. Many authors claim ILs to be green or environmentally friendly solvents, which explains some of the interest. The more reasonable point for using ILs for (inorganic) nanomaterials synthesis is that the very large number of different ILs should in principle enable the specific and targeted synthesis of interesting new materials with advantageous properties. Moreover, ILs can in some cases enable the synthesis of materials that cannot be made via conventional processes [21, 25, 27–34].

Among others, metal nanoparticle formation in ILs and their application have attracted interest because many ILs efficiently stabilize nanoparticles under a variety of experimental conditions. The particular interest in ILs is that they can also stabilize inorganics (not only nanoparticles) that cannot be stabilized otherwise. For example, Migowski et al. [35] have prepared nickel nanoparticles.

Endres et al. [22, 23, 36, 37] have electrodeposited germanium, aluminum, and tantalum from ILs. The same authors have used plasma chemistry for the synthesis of copper nanoparticles [38] and Janiak et al. [39–41] have reported on the synthesis of transition metal nanoparticles such as molybdenum from the corresponding metal carbonyl complexes.

While the above processes are efficient and often yield single phase materials, it has so far not been possible to deposit titanium (nanoparticles) from ILs. Endres et al. [42] have published a first account on this phenomenon, but so far the issue is unresolved. The current report focuses the chemical (not electrochemical) reduction of titanium alkoxides in several ILs in an attempt to synthesize titanium nanoparticles via a wet chemical pathway. Specifically, we have studied the chemical reduction of titanium(IV) from titanium isopropoxide with $NaBH_4$ in a series of imidazolium-based ILs. Interestingly, the results are in line with those reported by Endres et al. [42] in that the formed nanoparticles are not Ti(0) but various types of titanium oxides.

Results and discussion

Nanoparticles have been synthesized via the decomposition of titanium isopropoxide in a number of ILs. The reactions were performed under reducing conditions in the presence of $NaBH_4$ and at elevated temperatures to obtain homogeneous reaction mixtures, see "Experimental" for details. Typical sample color after precipitation is orange to light brown.

Figure 1 shows representative UV/Vis and IR spectra of some samples after isolation. IR spectroscopy shows that even after centrifugation and washing, quite a number of bands appear. The bands between ca. 3,200 and 2,900 cm^{-1} along with the bands between 1,600 and 1,500 cm^{-1} can be assigned to C–H stretching and in-plane vibrations of the imidazolium ring. The bands between 1,300 and 1,050 cm^{-1} can be assigned to aliphatic in-plane vibrations, and the bands between 900 and 750 cm^{-1} are due to the respective out of plane vibrations of the organic cations, respectively. Because of the rather large number of bands, it is difficult to determine whether or not there are also Ti–O vibrations visible in the IR spectra. In summary, however, IR spectroscopy suggests that even after extensive washing, some IL is adsorbed on the particles.

UV/Vis spectroscopy shows the same two features in all samples. Between ca. 200 and 240 nm, a rather intense and broad absorption band is visible and a second, much weaker absorption is visible between ca. 280 and 300 nm. The absorption between 200 and 240 nm is assigned to the imidazolium cation, which dominates the spectrum, again

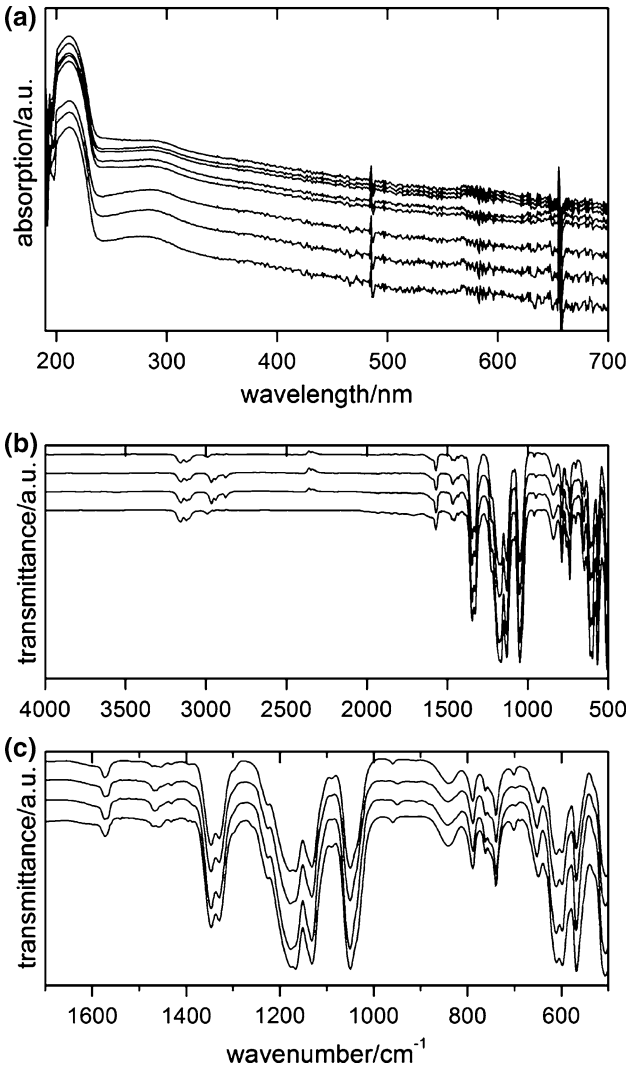

Fig. 1 IR and UV/Vis spectra of select samples. **a** UV/Vis spectra of (*from top to bottom*) nanoparticles grown in [Bmim][BF_4] at 120 °C, [Bmim][BF_4] at 180 °C, [Bmim][$N(Tf)_2$] at 160 °C, [Bmim][$N(Tf)_2$] at 180 °C, [Emim][$N(Tf)_2$] at 160 °C, [Emim][$N(Tf)_2$] at 180 °C, [Bmim][TfO] at 180 °C, [Bmim][TfO] at 140 °C. The spectra are displayed with a logarithmic *y*-axis for better visibility of the small absorption peaks at around 290 nm. **b**, **c** IR spectra of (*from top to bottom*) nanoparticles grown in [Bmim][$N(Tf)_2$] at 180 °C, [Bmim][$N(Tf)_2$] at 160 °C, [Emim][$N(Tf)_2$] at 180 °C, [Emim][$N(Tf)_2$] at 160 °C. **c** Magnified view of the same spectra showing the region between 1,700 and 500 cm^{-1}. Spectra are shifted vertically for clarity

even after extensive washing. The second, much weaker absorption maximum can be assigned to the nanoparticles. UV/Vis spectroscopy thus confirms the formation of nanoparticles, but the breadth of the peak also suggests that the size distribution of the particles is rather broad.

Figure 2 shows a representative Raman spectrum of a sample grown in [Emim][TfO]. The Raman spectrum shows four intense bands at 211, 398, 514, and 641 cm^{-1} that can be assigned to anatase [43–45].

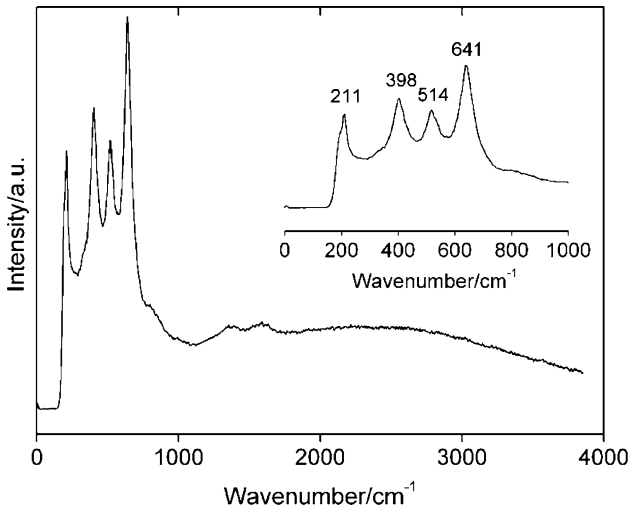

Fig. 2 Raman spectrum of precipitate in [Emim][TfO] at 140 °C. *Inset* is a magnified view of the low wavenumber region

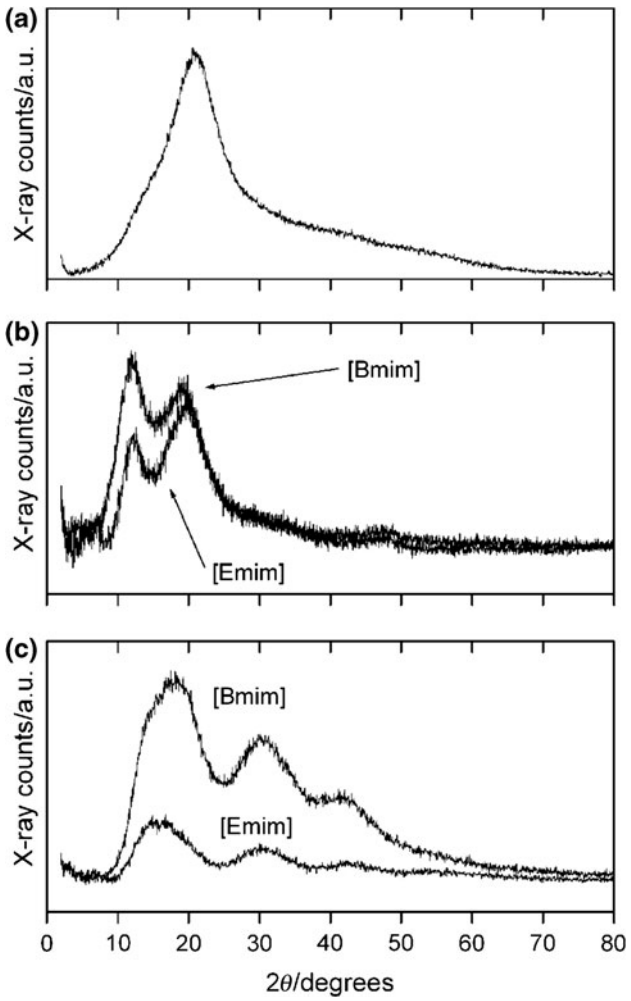

Fig. 3 XRD patterns of precipitates grown **a** in [Emim][BF_4] at 120 °C, **b** in [Emim][$N(Tf)_2$] and [Bmim][$N(Tf)_2$] at 140 °C, and **c** in [Emim][TfO] and [Bmim][TfO] at 140 °C

Figure 3 shows representative X-ray diffraction (XRD) patterns of the precipitates. Generally, broad and poorly resolved patterns are observed, but there are distinct differences between the anions. In the case of [Emim][MS], the XRD patterns have a poor signal to noise ratio. In the case of nanoparticles grown in the tetrafluoroborate [BF_4] ILs, one broad hump at ca. 21° 2θ is observed, occasionally with a shoulder at ca. 15°. With the [$N(Tf)_2$] ILs, two humps instead of one are observed and their centers are at ca. 12° and 19° 2θ. Finally, the patterns of the samples grown in the [TfO] ILs have the most complex shape, as here several broad humps at ca. 18°, 30°, 41°, and 56° 2θ are observed. Occasionally, also a shoulder at ca. 14° 2θ is observed here. As a result, there is somewhat of a discrepancy between the Raman and the XRD data, as there is no evidence for the presence of anatase in the XRD data.

Finally, it has to be noted that in some cases weak reflections that could be assigned to Ti(II)O could also be observed. These observations have, however, been inconclusive and complementary electron paramagnetic resonance (EPR) spectroscopy has not provided evidence of the presence of Ti(II) species and the corresponding XRD signals should thus be interpreted with care.

Figure 4 shows representative transmission electron microscopy (TEM) images of some samples. In general, two different types of precipitates can be distinguished. Similar to the XRD data, there is no significant difference between the [Emim] and [Bmim] cation, but the anions have quite a strong effect on the particle formation and aggregation process, similar to a recent report on gold nanoparticles in ILs [46].

[BF_4]- and [MS]-based ILs lead to well-defined, porous-looking, and roughly spherical aggregates with a diameter of ca. 50 nm. The particles grown in [BF_4] ILs appear a little denser than the particles grown in [MS] ILs, which look somewhat fluffier, but this is difficult to quantify. TEM suggests that these particles could form via the aggregation of smaller particles as in some cases particles with a diameter of ca. 5–10 nm can be observed. This observation can, however, not be made in all aggregates. In some cases, TEM also suggests that the particles are in fact larger structures that form via the growth of short needle-like elements from a central particle. In any case, the [BF_4] and [MS] anions lead to particles with rather complex shapes. This is in contrast to the effect of the ILs based on the [NTf_2] and [TfO] anions.

With [NTf_2] and [TfO] anions, large aggregates of smaller particles can be seen in the TEM images. The small primary particles are spherical and have a diameter of ca. 5–10 nm. Unlike the previous two samples, these samples do not have well-defined larger particle or aggregate shapes

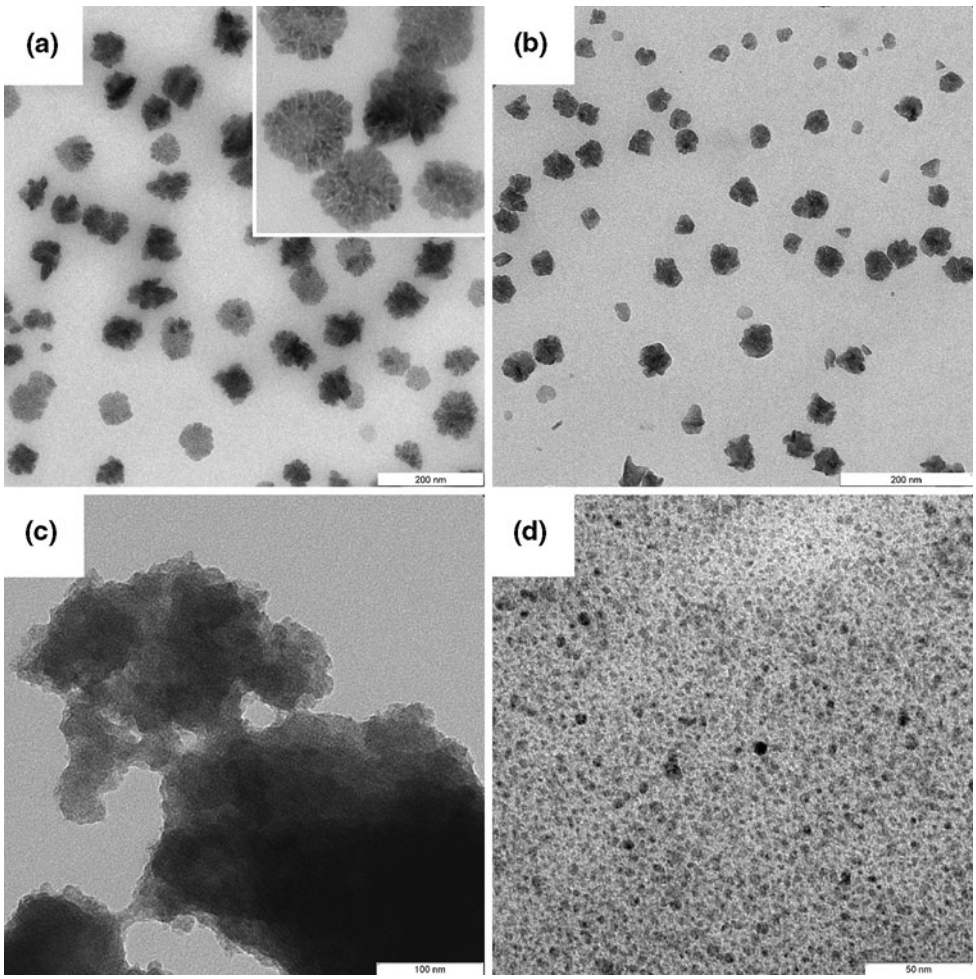

Fig. 4 Representative TEM images of **a** nanoparticles grown in [Emim][MS] at 140 °C, **b** [Bmim][BF_4] at 180 °C, **c** [Emim][TfO] at 140 °C, and **d** [Bmim][$N(Tf)_2$] at 180 °C. *Scale bars* are 200 nm (**a**, **b**), 100 nm (**c**), and 50 nm (**d**)

and sizes. Rather, there appear to be primary nanoparticles, which aggregate into relatively large, but poorly ordered structures. Unfortunately, attempts at obtaining high resolution TEM (HRTEM) images to confirm the Raman or XRD data failed, most likely due to the rather thick IL layer that is still present in the samples after isolation.

In order to better evaluate the composition of the nanoparticles, elemental analysis experiments have been performed. They have, however, been inconclusive, most likely due to the rather large fluorine content in the samples (from the ILs). In contrast, thermogravimetric analysis (TGA) provides quantitative insight into the decomposition process of the nanoparticulate samples (Fig. 5). TGA shows a slow weight loss between 25 and ca. 350 °C (13%), followed by a large, single-step weight loss between 350 and 550 °C (71%). Thereafter the TGA curve shows only a flat line at a residual mass of 15%.

The current study is an investigation on the formation of titanium nanoparticles from titanium isopropoxide under reducing and quasi-ionothermal conditions. UV/Vis spectroscopy (Fig. 1) and TEM (Fig. 4) show that the precipitates are indeed nanoparticles. However, Raman

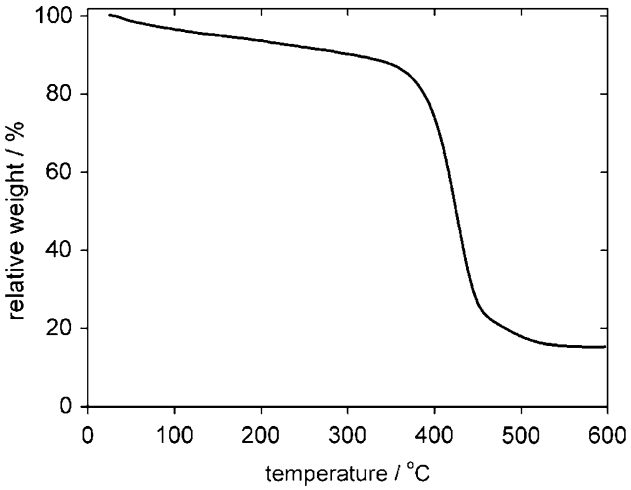

Fig. 5 Representative TGA curve of titania grown in [Emim][TfO] at 140 °C

spectroscopy (Fig. 2) and XRD (Fig. 3) show that, similar to an earlier electrochemical approach [42], chemical reduction does not produce titanium nanoparticles. Rather, Raman and XRD data suggest that the precipitates are

either anatase or amorphous TiO_2, both of which have been reported to form in ILs before [21, 42, 47–50]. Interestingly, however, Raman has in the current study shown no evidence for the formation of rutile, another TiO_2 crystal form, which has also been synthesized in ILs [21, 51].

Endres et al. [42] have attempted the electrodeposition of titanium, but have, apparently, failed so far and made oxygen-containing species instead. This has been assigned to the unfavorable interplay of the redox potentials and the stability of some intermediate stages, which prevent the formation of stable Ti deposits under the conditions studied so far. The current study confirms this earlier work in the sense that only oxidized species could also be found here. In the current case, we may argue that lower reaction temperatures could improve the situation, but even temperatures as low as 30 °C did not show any Ti(0) and only led to more heterogeneous mixtures and less controlled reaction conditions. We thus conclude that stronger reducing agents or other precursors, which are less prone to oxidation, could be favorable for the synthesis of titanium nanoparticles.

TEM (Fig. 4) shows that the nature of the IL anion has one significant effect. While in all samples the primary particles are roughly of the same size, the particle assembly is strikingly different. This shows, similar to earlier studies [21, 42, 47–51], that the anion restricts the growth of the titania nanoparticles to about 5–10 nm, but also that the colloidal stabilization of the individual particles is different in different ILs.

TGA (Fig. 5) shows that although the samples were extensively washed after synthesis, they have a rather large affinity for the IL, as a significant fraction of organic matter is still found in the isolated and purified samples. About 15–20% of the precipitates are rather easily removed from the sample, as indicated by the linear weight loss between 25 and ca. 350 °C. This weight loss is due to a combination of solvent (water adsorbed from the air, possibly traces of washing solvent) loss and an initial decomposition of the IL. The subsequent large loss of material can be assigned to the final decomposition ("burning") [52] of the IL adsorbed on the nanoparticles. TGA thus demonstrates that the IL is stabilized via adsorption on the particles, because the decomposition temperature is somewhat higher than for the pure ILs. TGA also shows that (consistent with IR and the intense UV/Vis absorption at ca. 200 nm, Fig. 1) the samples consist of a large fraction of organic (ca. 80%, Fig. 5) even after washing, which indicates a strong interaction between the inorganic particles and the IL. This observation is consistent with the TEM data (Fig. 4) and with earlier reports [21, 42, 47–51], both of which suggest a rather strong interaction between the IL and the precipitate.

In summary, the current study thus shows that the synthesis of titanium nanoparticles in IL remains elusive, mostly due to the fact that the formation of presumably amorphous or oxidized species (Fig. 2, 3) dominates the nanoparticle formation. IR, UV/Vis (Fig. 1), TEM (Fig. 4), and TGA (Fig. 5) indicate that the interaction between the particles and the ILs is so strong that ca. 80 wt% of the final product are IL or IL fragments.

Conclusion

The current study explores the potential of ILs for the synthesis and stabilization of titanium nanoparticles under reducing conditions. Similar to electrochemical approaches [42], however, chemical reduction processes also appear to be unsuccessful. In all cases, yellowish precipitates form, but they are either amorphous titanium oxides or possibly anatase. No evidence for the formation of metallic titanium has been observed. The report thus shows that even reducing conditions produce oxidized titanium species. They are, however, difficult to characterize, but clearly illustrate that the chemical synthesis of titanium nanoparticles in ILs remains elusive and further investigation into the topic is necessary.

Experimental

Materials

ILs based on 1-ethyl-3-methylimidazolium (Emim) or 1-butyl-3-methylimidazolium (Bmim) cations and methanesulfonate (MS), tetrafluoroborate (BF_4), trifluoromethanesulfonate (TfO), bis(trifluoromethylsulfonyl)imide (NTf_2), and ethylsulfate (ES) anions were purchased from IoLiTec (Freiburg, Germany) and used as received. Water content in all ILs was between 0.001 and 0.1% (v/v), as determined by volumetric Karl Fischer titration.

Nanoparticle synthesis

In a typical synthesis, 0.0994 g (0.355 mmol) of $Ti[OCH(CH_3)_2]_4$ was added to 5 cm^3 of IL. The mixture was sonicated for 10 min. Then 0.0038 g (1 mmol) of $NaBH_4$ was added at ambient conditions. The resulting colorless solution was heated to between 140 and 180 °C for 12 h. Before isolating the precipitate by centrifugation, a small fraction of the orange or light brown colloidal dispersion was removed for UV/Vis, IR, and Raman measurements. The centrifuged product was washed with ethanol and dried under vacuum at room temperature for 12 h. Control experiments were also performed at 30 °C.

X-ray diffraction

Wide angle X-ray diffraction (XRD) was done on an ENRAF-Nonius FR 590 diffractometer with a Cu K_α X-ray

tube fitted with an Inel CPS 120 hemispherical detector ranging from 1 to 120° 2θ. Data analysis was performed via EVA.

Spectroscopy

FTIR spectra of the solid samples were also recorded with KBr pellets in the same spectral range on a Thermo Nicolet Nexus 670 spectrometer at 2 cm^{-1} resolution. UV/Vis spectroscopy was done on an Agilent 8453 spectrometer using 10-mm quartz cuvettes containing the nanoparticle dispersion either in the as-synthesized dispersion or redispersed particles in ethanol at room temperature. EPR spectra were recorded on a Bruker CW-EPR spectrometer E500 in X-band (ca. 9.5 GHz) between 100 and 295 K.

Electron microscopy

TEM images were acquired on a Zeiss EM 912 operated at 120 kV. One droplet of the suspension was applied to a 400-mesh carbon-coated copper grid and left to dry in air.

Thermogravimetric analysis

TGA was done on a Mettler Toledo TGA/SDTA851e from 25 to 600 °C with heating rates of 10 °C/min under nitrogen (10 cm^3/min) in alumina crucibles.

Acknowledgments We thank H. Runge and R. Pitschke for SEM and TEM measurements, Prof. H.-J. Holdt and Dr. K. Tauer for access to their spectrometers, and I. Zenke for help with XRD. A. A. Ayi acknowledges the DAAD for a research fellowship and the University of Calabar for a research leave. Further funding from the University of Potsdam and the MPI of Colloids and Interfaces (Colloid Chemistry Department) is gratefully acknowledged.

References

1. Caruso F (ed) (2004) Colloids and colloid assemblies. Wiley-VCH, Weinheim
2. Matsunaga T, Okamura T, Tanaka T (2004) J Mater Chem 14:2099
3. Matsunaga T, Suzuki T, Tanaka M, Arakaki A (2007) Trends Biotechnol 25:182
4. Mornet S, Vasseur S, Grasset F, Duguet E (2004) J Mater Chem 14:2161
5. Millstone JE, Hurst SJ, Metraux GS, Cutler JI, Mirkin CA (2009) Small 5:646
6. Na HB, Song I-C, Hyeon T (2009) Adv Mater 21:2133
7. Niederberger M (2007) Acc Chem Res 40:793
8. Pinna N, Niederberger M (2008) Angew Chem Int Ed 47:5292
9. Garnweitner G, Niederberger M (2008) J Mater Chem 18:1171
10. Xu AW, Antonietti M, Yu SH, Cölfen H (2008) Adv Mater 20:1333
11. Meldrum FC, Cölfen H (2008) Chem Rev 108:4332
12. Cölfen H (2008) Angew Chem Int Ed 47:2351
13. Kulak AN, Iddon P, Li Y, Armes SP, Colfen H, Paris O, Wilson RO, Meldrum FC (2007) J Am Chem Soc 129:3736
14. Niederberger M, Cölfen H (2006) Phys Chem Chem Phys 8:3271
15. Cooper ER, Andrews CD, Wheatley PS, Webb PB, Wormald P, Morris RE (2004) Nature 430:1012
16. Parnham ER, Morris RE (2007) Acc Chem Res 40:1005
17. Morris RE (2008) Angew Chem Int Ed 47:443
18. Taubert A (2005) Acta Chim Slov 52:183
19. Taubert A (2008) Inorganic nanomaterials synthesis using ionic liquids. In: Lukehart CM, Scott RA (eds) Nanomaterials: inorganic and bioinorganic perspectives. Wiley, New York, pp 369–380
20. Antonietti M, Kuang D, Smarsly B, Zhou Y (2004) Angew Chem Int Ed 43:4988
21. Kaper H, Endres F, Djerdj I, Antonietti M, Smarsly BM, Maier J, Hu Y-S (2007) Small 3:1753
22. Endres F (2002) Proc Electrochem Soc 2002–19:677
23. Moustafa EM, Zein El Abedin S, Shkurankov A, Zschippang E, Saad AY, Bund A, Endres F (2007) J Phys Chem B 111:4693
24. Zein El Abedin S, Endres F (2006) ChemPhysChem 7:58
25. Armand M, Endres F, MacFarlane DR, Ohno H, Scrosati B (2009) Nat Mater 8:621
26. Endres F, MacFarlane D, Abbott A (eds) (2008) Electrodeposition from ionic liquids. Wiley-VCH, Weinheim
27. Nakashima T, Kimizuka N (2003) J Am Chem Soc 125:6386
28. Li Z, Rabu P, Strauch P, Mantion A, Taubert A (2008) Chem Eur J 14:8409
29. Taubert A (2005) Acta Chim Slov 52:168
30. Taubert A, Palivan C, Casse O, Gozzo F, Schmitt B (2007) J Phys Chem C 111:4077
31. Taubert A, Steiner P, Mantion A (2005) J Phys Chem B 109:15542
32. Soejima T, Kimizuka N (2005) Chem Lett 34:1234
33. Li Z, Jia Z, Luan Y, Mu T (2009) Curr Opin Solid State Mater Sci 12:1
34. Parnham ER, Wheatley PS, Morris RE (2006) Chem Commun 4:380
35. Migowski P, Machado G, Texeira SR, Alves MCM, Morais J, Traverse A, Dupont J (2007) Phys Chem Chem Phys 9:4814
36. Liu QX, El Abedin SZ, Endres F (2008) J Electrochem Soc 155:D357
37. Ispas A, Adolphi B, Bund A, Endres F (2010) Phys Chem Chem Phys 12:1793
38. Brettholle M, Hofft O, Klarhofer L, Mathes S, Maus-Friedrichs W, El Abedin SZ, Krischok S, Janek J, Endres F (2010) Phys Chem Chem Phys 12:1750
39. Redel E, Thomann R, Janiak C (2008) Inorg Chem 47:14
40. Redel E, Thomann R, Janiak C (2008) Chem Commun 15:1789
41. Kramer J, Redel E, Thomann R, Janiak C (2008) Organometallics 27:1976
42. Endres F, Zein El Abedin S, Saad AY, Moustafa EM, Borissenko N, Price WE, Wallace GG, MacFarlane DR, Newman PJ, Bund A (2008) Phys Chem Chem Phys 10:2189
43. Farmer VC (1975) The infrared spectra of minerals. Mineralogical Society, London
44. Cheng H, Ma J, Zhao Z, Qi L (1995) Chem Mater 7:663
45. Tompsett GA, Bowmaker GA, Cooney RP, Metson JB, Rodgers KA, Seakins JM (1995) J Raman Spectrosc 26:57
46. Khare V, Li Z, Mantion A, Ayi AA, Sonkaria S, Voelkel A, Thünemann AF, Taubert A (2010) J Mater Chem 20:1332
47. Paramasivam I, Macak JM, Selvam T, Schmuki P (2008) Electrochim Acta 54:643
48. Al Zoubi M, Farag HK, Endres F (2008) Aust J Chem 61:704
49. Farag HK, Al Zoubi M, Endres F (2009) J Mater Sci 44:122
50. Liu YH, Lin CW, Chang MC, Shao H, Yang AC-M (2008) J Mater Sci 43:5005
51. Zhai Y, Zhang Q, Liu F, Gao G (2008) Mater Lett 62:4563
52. Li Z, Friedrich A, Taubert A (2008) J Mater Chem 24:1008